Description and Evaluation of the Characteristics of the NCAR High-Resolution Land Data Assimilation System

FEI CHEN,* KEVIN W. MANNING,* MARGARET A. LEMONE,* STANLEY B. TRIER,* JOSEPH G. ALFIERI,+ RITA ROBERTS,* MUKUL TEWARI,* DEV NIYOGI,# THOMAS W. HORST,* STEVEN P. ONCLEY,* JEFFREY B. BASARA,@ AND PETER D. BLANKEN+

*National Center for Atmospheric Research,& Boulder, Colorado
+University of Colorado, Boulder, Colorado
#Purdue University, West Lafayette, Indiana
@Oklahoma Climatological Survey, University of Oklahoma, Norman, Oklahoma

(Manuscript received 22 November 2005, in final form 9 June 2006)

ABSTRACT

This paper describes important characteristics of an uncoupled high-resolution land data assimilation system (HRLDAS) and presents a systematic evaluation of 18-month-long HRLDAS numerical experiments, conducted in two nested domains (with 12- and 4-km grid spacing) for the period from 1 January 2001 to 30 June 2002, in the context of the International H_2O Project (IHOP_2002). HRLDAS was developed at the National Center for Atmospheric Research (NCAR) to initialize land-state variables of the coupled Weather Research and Forecasting (WRF)–land surface model (LSM) for high-resolution applications. Both uncoupled HRDLAS and coupled WRF are executed on the same grid, sharing the same LSM, land use, soil texture, terrain height, time-varying vegetation fields, and LSM parameters to ensure the same soil moisture climatological description between the two modeling systems so that HRLDAS soil state variables can be used to initialize WRF–LSM without conversion and interpolation. If HRLDAS is initialized with soil conditions previously spun up from other models, it requires roughly 8–10 months for HRLDAS to reach quasi equilibrium and is highly dependent on soil texture. However, the HRLDAS surface heat fluxes can reach quasi-equilibrium state within 3 months for most soil texture categories. Atmospheric forcing conditions used to drive HRLDAS were evaluated against Oklahoma Mesonet data, and the response of HRLDAS to typical errors in each atmospheric forcing variable was examined. HRLDAS-simulated finescale (4 km) soil moisture, temperature, and surface heat fluxes agreed well with the Oklahoma Mesonet and IHOP_2002 field data. One case study shows high correlation between HRLDAS evaporation and the low-level water vapor field derived from radar analysis.

1. Introduction

This paper evaluates a land-state initialization technique for high-resolution coupled Weather Research and Forecast (WRF)–land surface model (LSM) numerical weather forecasts. Subjects discussed in this article include the concept of a high-resolution land data assimilation system (HRLDAS) based on the "Noah" land surface model, its configuration for nested grids, the time required for its spinup to reach quasi-equilibrium state, its sensitivity to various atmospheric forcing conditions, and its verification against observed profiles of soil moisture and temperature, surface heat fluxes, and radar-derived refractivity (i.e., low-level water vapor) fields.

According to experiments with operational models at numerical weather prediction (NWP) centers (Betts et al. 1997; Beljaars et al. 1996; Chen et al. 1997; Ek et al. 2003), the improvement in 1–5-day predictions of boundary layer development, cloud, precipitation, and surface meteorological conditions may rely on the land surface physics and initialization of land state (e.g., vegetation characteristics, soil moisture, and soil temperature). The important role of soil moisture in deep-convection development has also been recognized (Lanicci

& The National Center for Atmospheric Research is sponsored by the National Science Foundation.

Corresponding author address: Fei Chen, NCAR/RAL, P.O. Box 3000, Boulder, CO 80307-3000.
E-mail: feichen@ucar.edu

DOI: 10.1175/JAM2463.1

et al. 1987; Pielke and Zeng 1989; Ziegler et al. 1997; Shaw et al. 1997; Chen et al. 2001; Trier et al. 2004). Routine soil moisture profile observations at high horizontal resolution simply do not exist on regional and global areas. Furthermore, the heterogeneity in topography, soil, and vegetation characteristics frequently occurs at small scales, further complicating the use of the traditional "point" measurements of soil moisture at the spatial scales typical of NWP models.

A number of studies have attempted to estimate soil moisture profiles down to depths beyond the penetration of remote sensing observations (Jackson 1980, 1997; Camillo and Schmugge 1983) and used remotely sensed surface characteristics to constrain unrealistic simulated soil moisture (e.g., Entekhabi et al. 1994; Houser et al. 1998; Walker and Houser 2001). The ultimate solution for NWP land-state initialization probably lies in combining data assimilation techniques, satellite-derived soil data, and land surface models, but an intermediate step is to use observed rainfall, satellite-derived surface insolation, and meteorological analyses to drive an uncoupled (offline) integration of an LSM, so that the evolution of modeled soil moisture can be constrained by observed forcing conditions. A North American land data assimilation system (NLDAS; Mitchell et al. 2004) that consists of four LSMs using common hourly surface forcing has already been developed, and the NLDAS component using the Noah LSM with ⅛° resolution is being developed at the National Centers for Environmental Prediction (NCEP) as an experimental product. However, NLDAS may not be an optimal solution for high-resolution WRF applications, which routinely use a grid spacing of 2–4 km. Even with the same baseline Noah LSM in both WRF–Noah and NLDAS–Noah modeling systems, it may be problematic to use soil moisture obtained from one LDAS to initialize a coupled modeling system that is executed with different grid configurations (and hence different model resolution), because there is a mismatch in terrain, land use, and soil texture between these two different modeling systems, which can result in different soil moisture climatological values.

Therefore, HRLDAS is being developed at the National Center for Atmospheric Research (NCAR) to address these issues and to meet the demand for accurate land-state initialization. In essence, HRLDAS is executed, in uncoupled mode like NLDAS, on the same WRF nested grids, so that the coupled WRF and uncoupled HRLDAS share the same Noah land surface model, land use, soil texture, terrain height, time-varying vegetation properties, and LSM parameters. Hence, the HRLDAS soil conditions can be directly ingested into the coupled WRF–Noah model without interpolation. Recent, collective efforts were devoted to the evaluation of the multi-LSM-based NLDAS (Cosgrove et al. 2003; Robock et al. 2003; Pinker et al. 2003; Luo et al. 2003; Schaake et al. 2004; Mitchell et al. 2004). Our research consists of evaluating a new framework to initialize land-state variables for the coupled WRF–Noah modeling system running with a nested domain (vs the single-grid ⅛° NLDAS approach) with a long-term (1 January 2001–30 June 2002) HRLDAS run. In this paper, we focus on a few unique aspects that were not fully explored in aforementioned NLDAS efforts:

1) evaluation of the 4-km hourly NCEP stage-IV rainfall analysis (in contrast to the ¼° gauge-based rainfall used in NLDAS),
2) analysis of the spinup dependency of HRLDAS (which was initialized by model-analyzed soil moisture rather than by random soil moisture used in previous spinup studies) on soil texture using surface fluxes as equilibrium criteria,
3) evaluation of HRLDAS fields (soil moisture, soil temperature, and surface fluxes) at 4-km scales, and
4) systematic analysis of HRLDAS sensitivity to each atmospheric forcing variable.

We describe the general characteristics of HRLDAS and the data used for its validation in section 2. Issues concerning spinup of this soil assimilation system, its sensitivity to errors in atmospheric forcing variables, and its verification are presented in section 3, followed by a summary.

2. Description of high-resolution land data assimilation system and data used

a. The Noah land surface model

The heart of the HRLDAS infrastructure is the Noah LSM (Chen and Dudhia 2001; Ek et al. 2003). This LSM and its previous version, known as the Oregon State University (OSU) LSM (Pan and Mahrt 1987; Chen et al. 1996; Chen and Dudhia 2001), has been implemented in the fifth-generation Pennsylvania State University–NCAR Mesoscale Model (MM5) and the WRF model (Tewari et al. 2005). A major community effort has been undertaken among NCAR, NCEP, the U.S. Air Force Weather Agency (AFWA), and the university community to develop and implement a unified Noah LSM, which is an enhanced version of the OSU/Noah LSM (Ek et al. 2003). The Noah LSM is based on coupling of the diurnally dependent Penman potential evaporation approach of Mahrt and Ek (1984), the multilayer soil model of Mahrt and Pan (1984), and the primitive canopy model of Pan and Mahrt (1987). It has

been extended by Chen et al. (1996) to include the modestly complex canopy resistance approach of Noilhan and Planton (1989) and Jacquemin and Noilhan (1990) and by Koren et al. (1999) to include frozen ground physics. Recent updates to the Noah LSM include new treatment of soil thermal conductivity and ground heat flux for wet soils and snowpack, as well as improvement to the formulation of bare-soil evaporation (Ek et al. 2003), a simple urban land use treatment, and seasonal variability of surface emissivity (Tewari et al. 2005).

As used in the uncoupled HRLDAS and in the coupled WRF model, the Noah LSM has one canopy layer and the following prognostic variables: total volumetric soil moisture and volumetric liquid soil moisture (not soil ice, which is obtained from the difference of predicted states of total soil moisture minus liquid soil moisture), soil temperature in four soil layers, water stored on the canopy, bulk snowpack density, snow albedo, and snow stored on the ground. For the soil model to capture the daily, weekly, and seasonal evolution of soil moisture and also to mitigate the possible truncation error in discretization, we used four soil layers in HRLDAS; the thicknesses of the layers (listed from the surface to deeper in the ground) are 0.1, 0.3, 0.6, and 1.0 m, although the Noah LSM can be configured to run with more than four layers. The total soil depth is 2 m, and the vegetation root depth varies as a function of land use types in the upper 1.5 m of soil. Seasonal variations in green vegetation fraction are based on monthly 0.15°, 5-yr climatological, and satellite Advanced Very High Resolution Radiometer/normalized difference vegetation index (NDVI) data (Gutman and Ignatov 1998).

b. High-resolution land data assimilation system configuration

Today's NWP models are often executed with a grid spacing of 1–10 km and need to capture heterogeneity of soil and vegetation at such scales. Running an LDAS at finescale (e.g., 1 km) and covering a large domain is computationally demanding. Hence, the concept of nested grids is used in HRLDAS to reduce the computational requirement and to ensure the consistency with the WRF–Noah coupled system. HRLDAS is essentially an uncoupled land surface modeling system that integrates finescale static surface fields (e.g., land use and soil texture maps), time-varying vegetation characteristics (e.g., green vegetation fraction) derived from satellite, observed rainfall and solar downward radiation at the surface, and observed or analyzed near-surface weather variables to drive the Noah LSM to simulate long-term evolution of land-state variables (e.g., soil moisture and temperature profiles). Despite the "A" in HRLDAS meaning assimilation, the current HRLDAS does not perform data assimilation in the classic sense. HRLDAS is so named to follow the widely accepted LDAS concept and terminology as used, for instance, in NLDAS by Mitchell et al. (2004). Nevertheless, it is expected that the LDAS framework (e.g., NLDAS and HRLDAS) will allow actual data assimilation using such methods as adjoint models and Kalman filtering.

The most important consideration for the uncoupled HRLDAS configuration is to ensure its complete compatibility with the WRF–Noah coupled model. First, the WRF "Standard Initialization" (SI) program was run to generate nested grids. In this paper, as an example, WRF SI is set up to run on two grids: the inner grid with 4-km grid spacing and the outer grid with 12-km grid spacing for the central United States (see Fig. 1). This domain was selected for the readily available forcing and verification data in this region. Second, HRDLAS reads the WRF SI output file that contains grid configuration (resolution, grid points, and projection), terrain height, land–water masks, land use and soil texture maps, and monthly vegetation fields temporally interpolated to the yearday of the valid simulation time and assigns these surface fields to each grid point of HRLDAS. In addition, all vegetation and soil parameters required by Noah are specified by the same lookup tables shared by WRF and HRLDAS. Hence, there is no difference in the surface fields and Noah parameters between coupled WRF and uncoupled HRLDAS. Third, various atmospheric forcing conditions (see Table 1) are collected and interpolated to each HRLDAS grid point and used to drive the Noah LSM at each grid point of the two nested grids. In this example, HRLDAS has 290 × 248 grid points on the outer 12-km grid and 462 × 387 grid points on the inner 4-km grid and takes roughly 48 h of central processing unit (CPU) time on a single-CPU-based Linux personal computer to execute an 18-month-long simulation.

Note that the 4-km hourly NCEP stage-IV rainfall analysis based on rain gauge–calibrated Weather Surveillance Radar-1988 Doppler (WSR-88D) radar-rainfall estimates (Fulton et al. 1998), which is really a mosaic of National Weather Service River Forecast Center stage-III regional analyses, is used to drive HRLDAS, in contrast to the ¼° gauge-only daily precipitation that is temporally disaggregated to hourly by using stage-IV data in NLDAS (Mitchell et al. 2004). In Fig. 1b, the 4-km HRLDAS soil moisture field shows the general west-to-east soil moisture gradient, reflecting the large-scale rainfall pattern across the International H_2O Project (IHOP_2002) region, as well as fine-

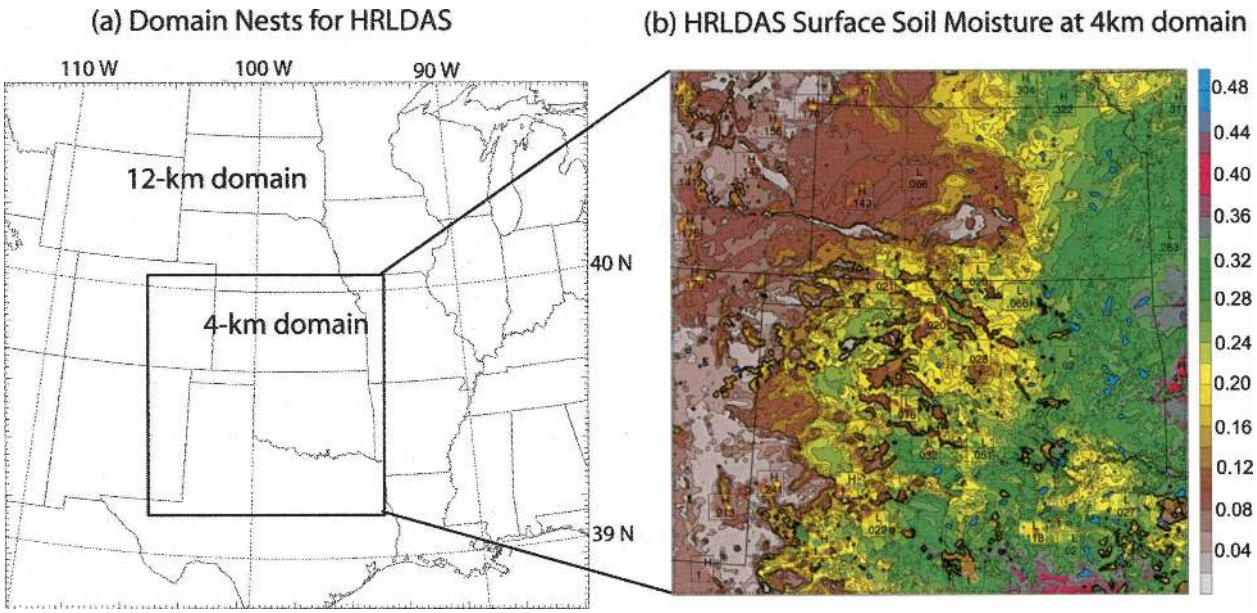

FIG. 1. Nested grids used for the HRLDAS IHOP_2002 experiment: (a) 12-km outer grid and 4-km inner grid and (b) HRLDAS surface volumetric soil moisture (contours in 0.02 m^3 m^{-3} intervals starting from 0.02 m^3 m^{-3}) valid at 1200 UTC 29 May 2002.

scale heterogeneity caused by small-scale convective rain in 4-km stage IV, land use types, soil texture, and vegetation characteristics.

c. Data from the IHOP_2002 field experiment

The principal objectives of IHOP_2002, conducted from 13 May to 25 June 2002 in the U.S. southern Great Plains (SGP), were to obtain an improved characterization of the time-varying three-dimensional water vapor field and to evaluate the use of these fields in improving the understanding and prediction of convective rainfall (Weckwerth et al. 2004). One important IHOP_2002 atmospheric boundary layer (ABL) objective was to investigate the evolution of evaporation over different land use types during the growing season and to determine its effect on the thermodynamic structure of the ABL. Ten flux-tower stations (nine by NCAR and one by the University of Colorado) were placed strategically along three boundary layer–heterogeneity-mission flight tracks flown by the University of Wyoming King Air (Fig. 2) and over various land use types (see Table 2) that include winter wheat (sites 5 and 6), grassland (sites 2, 4, 7, 8, and 9), sparsely vegetated sagebrush (site 3), heavily grazed grass (site 10), and bare ground (site 1) across the strong precipitation gradient between eastern Kansas and the Oklahoma Panhandle.

The 10 flux-tower stations provide downward solar and longwave radiation, reflected solar radiation, upward longwave radiation, sensible heat flux, latent heat flux, and ground heat flux. They also measure near-surface meteorological conditions, along with soil moisture and temperature at 5 cm. To enable definitive testing and improvement of LSMs, the nine NCAR flux-tower stations were enhanced with soil profiles down to 70–90 cm to measure soil moisture, matric potential, and temperature continually at six soil depths. Also measured 3–4 times during IHOP_2002 were vegetation characteristics such as plant height, NDVI, leaf area index (LAI), canopy temperature, and stomatal conductance. All continuous data were stored as 5-min block averages and then quality checked and postprocessed using a standard suite of corrections that includes a sonic coordinate rotation (Wilczak et al. 2001), the Webb–Pearman–Leuning correction for the effects of density and buoyancy on the moisture flux (Webb et al. 1980), and a correction for the spatial separation of the krypton hygrometer (KH2O) and sonic anemometer (Horst 2006). The IHOP_2002 surface radiation and heat flux measurements, which are not available from the Oklahoma Mesonet stations, are used in this paper to evaluate HRLDAS.

The IHOP-station latent heat fluxes were computed from sonic anemometer and KH2O data using the eddy correlation method. The electronics for several of the KH2O sensors had water infiltration problems, which were fixed during the project. The data were hand edited to remove cases in which failure was obviously detected, but the current data of latent heat fluxes, par-

TABLE 1. Data used in HRLDAS.

Data	Sources	Interpolation method
Surface fields		
Land use	WRF SI output or WRF input based on 30-s U.S. Geological Survey (USGS) 24 categories (Loveland et al. 1995)	No interpolation from WRF grid to HRLDAS gird; aggregate to a single dominant type for each grid box in WRF
Soil texture	WRF SI output or WRF input based on hybrid 30-s State Soil Geographic Database (STATSGO, now referred to as the U.S. General Soil Map) (for CONUS) and 5-min Food and Agriculture Organization (outside CONUS) 16-category soil texture (Miller and White 1998)	No interpolation from WRF grid to HRLDAS gird; aggregate to a single dominant type for each grid box in WRF
Green vegetation fraction	WRF SI output or WRF input based on 0.15° monthly satellite-derived green vegetation fraction (Gutman and Ignatov 1998)	No interpolation from WRF grid to HRLDAS gird; bilinear interpolation from 0.15° regular lat/lon grid to WRF grid
Terrain height	WRF SI output or WRF input based on USGS-derived 30-s topographical height data	No interpolation from WRF grid to HRLDAS gird; bilinear interpolation in WRF grid
Vegetation and soil parameters required by the Noah LSM	Parameters are specified to each land use and soil texture category using lookup tables (Chen and Dudhia 2001)	
Atmospheric forcing		
Precipitation	4-km hourly NCEP stage-IV rainfall analyses based on rain gauge–calibrated WSR-88D radar-rainfall estimates (Fulton et al. 1998)	Mass conservation interpolation
Downward solar radiation	The 0.5° hourly downward solar radiation derived from the GOES, a product jointly developed by the National Environmental Satellite, Data and Information Service and the University of Maryland (Pinker et al. 2003)	Bilinear
Downward longwave radiation, 10-m wind speed, 2-m temperature and specific humidity, and surface pressure	Three-hourly atmospheric analyses from the NCEP EDAS (Rogers et al. 1995)	Linear interpolation to hourly and bilinear interpolation in space

ticularly at sites 7, 8, and 9, were contaminated by this problem. The KH2O data at the nine NCAR stations also were contaminated by the radio-frequency transmission of the station data to the Geostationary Operational Environmental Satellite (GOES) for approximately 20 s every 5 min. The error in the computed water vapor fluxes from this contamination is estimated to be negligible, because the noise was not correlated with vertical velocity. Thus, despite the above-mentioned problems, we expect reasonable water vapor fluxes in the final dataset.

d. Oklahoma Mesonet data

The HRLDAS-simulated soil moisture of April–June 2002 was verified against soil moisture measurements from the Oklahoma Mesonet. In addition, the majority of atmospheric forcing variables used in HRLDAS were verified against mesonet meteorological observations. The Oklahoma Mesonet is an automated network of 116 remote, meteorological stations across Oklahoma (Brock et al. 1995; Shafer et al. 2000). Each station measures air temperature and relative humidity at 1.5 m, wind speed and direction at 10 m, atmospheric pressure, incoming solar radiation, rainfall, and bare and vegetated soil temperatures at 10 cm below ground level. Additional information concerning the Oklahoma Mesonet was located online at the time of writing (http://www.mesonet.org). Between 1996 and 1999, heat dissipation sensors were installed at 101 mesonet stations to provide real-time observations of soil moisture (Basara and Crawford 2000, 2002) at depths of 5, 25, 60, and 75 cm. Soil temperature is measured at depths of 5, 10, and 25 cm using a stainless steel encased thermistor that has an accuracy of 0.5°C from −20° to 50°C (Brock et al. 1995).

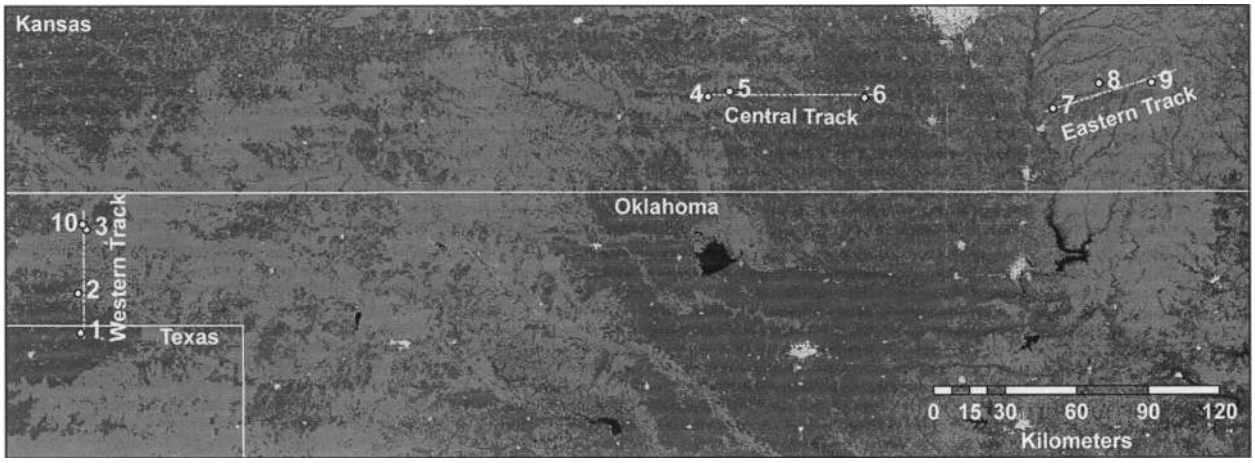

FIG. 2. Locations of the nine NCAR IHOP_2002 (1–9) and University of Colorado (10) flux-tower stations with soil moisture and temperature measurement array. Also shown are three flight tracks of the University of Wyoming King Air aircraft. Light-gray shaded areas represent urban land use, medium gray is grassland/shrub land, dark gray is cropland, and black is open water.

3. Results and discussion

a. Spinup of HRLDAS land-state variables

Each individual LSM has its own climatological description, especially for soil moisture, depending on its treatment of physical processes and chosen parameter values. The study by Koster and Milly (1997), for example, shows that different LSMs exhibit substantially different climatological values of the annual mean of soil moisture and the amplitude of the seasonal change of soil moisture owing to differences in how the LSMs determine evaporation and runoff as functions of soil moisture. The length of time for an LSM to reach its preferred climatological state (or equilibrium state) from a set of initial conditions is referred to as spinup time. A number of studies have examined this issue (Yang et al. 1995; Robock et al. 1998), which included a wide range of LSMs and analyzed simulations for single-vegetation-type and single-soil-type situations, as well as multiple grid points. Chen and Mitchell (1999) found that, based on results of Noah LSM global simulations with 1° grid spacing, the equilibrium condition was established within 3 yr over most areas. In some regions with a deep total soil layer and sparse vegetation, the equilibrium process took longer, because the evaporation is limited by slow water diffusion time scales between the surface and deep soil layers. Cosgrove et al. (2003) utilized two extreme soil moisture values (saturated and completely dry) together with soil moisture conditions obtained from NCEP–Department of Energy Global Reanalysis-2 to initialize three land surface models, including the Noah LSM, which ran for 11 yr, and found that these LSMs reach a state of rough equilibrium within the first 1–2 yr.

Our particular interests in soil moisture spinup are somewhat different from those LSM spinup studies—namely, given a set of soil conditions that already reflect recent history of precipitation but are obtained from a different source, how long does it take to spin up HRLDAS to obtain equilibrium soil conditions at small scales of sufficient quality for coupled LSM–NWP model simulations? The sources of these previously

TABLE 2. Land surface characteristics at each NCAR and CU station (site) for IHOP_2002.

Station	Nearby town	Lat (N)	Lon (W)	Elev (m MSL)	Land use	Surface soil texture
1	Booker, TX	36°28.370′	100°37.075′	872	Fallow	Sandy clay loam
2	Elmwood, OK	36°37.327′	100°37.619′	859	Grassland	Sandy clay loam
3	Beaver, OK	36°51.662′	100°35.670′	780	Sagebrush	Sandy loam
4	Zenda, KS	37°21.474′	98°14.679′	509	Grassland	Loam
5	Spivey, KS	37°22.684′	98°9.816′	506	Winter wheat	Loam
6	Conway Springs, KS	37°21.269′	97°39.200′	417	Winter wheat	Clay loam
7	New Salem, KS	37°18.792′	96°56.323′	382	Grassland	Silty clay loam
8	Atlanta, KS	37°24.418′	96°45.937′	430	Grassland	Silty clay loam
9	Grenola, KS	37°24.618′	96°34.028′	447	Grassland	Silty clay loam
10	Beaver, OK	36°52.800′	100°36.601′	786	Grassland	Sandy loam

TABLE 3. Configuration of HRLDAS spinup experiments. Note that the averaged statistics for June 2002 from each spinup experiment were used to compare with those from the control run. Each experiment was initialized with NCEP EDAS soil moisture and temperature valid at the starting time.

HRLDAS spinup expt	Starting time/date	Ending time/date	Spinup time (months) up to 1 Jun 2002
Control run	0000 UTC 1 Jan 2001	0000 UTC 1 Jul 2002	17
First spinup run	0000 UTC 1 Feb 2001	0000 UTC 1 Jul 2002	16
Second spinup run	0000 UTC 1 Mar 2001	0000 UTC 1 Jul 2002	15
Third spinup run	0000 UTC 1 Apr 2001	0000 UTC 1 Jul 2002	14
Fourth spinup run	0000 UTC 1 May 2001	0000 UTC 1 Jul 2002	13
⋮	⋮	0000 UTC 1 Jul 2002	⋮
15th spinup run	0000UTC 1 May 2002	0000 UTC 1 Jul 2002	1
Last (16th) spinup run	0000 UTC 1 Jun 2002	0000 UTC 1 Jul 2002	0

spunup soil conditions may include remotely sensed soil moisture data, a model/analysis system that has a coarse spatial resolution or employs different configurations of terrain, land use types, soil textures, or even a different LSM. These sources of model soil data could be, for example, uncoupled global LDAS [e.g., the AFWA Agricultural Meteorology Modeling System (AGRMET; Gayno and Wegiel 2000)] or regional LDAS like NLDAS or global coupled weather forecast models (e.g., NCEP Global Forecast System) or regional coupled forecast models [e.g., NCEP Eta Data Assimilation System (EDAS)].

It is reasonable to speculate that using these previously spunup soil conditions may require shorter spinup time than using extreme or arbitrary soil conditions. In the context of this HRLDAS simulation, we need accurate, finescale land-state conditions to initialize the coupled WRF–Noah LSM model to investigate 2002 June IHOP_2002 convective cases. Our approach is to use 40-km NCEP EDAS–Noah four-layer soil moisture and temperature to initialize HRLDAS and then to let HRLDAS, driven by high-resolution spatial pattern of land use, soil texture, and 4-km precipitation, develop small-scale heterogeneities. To address the spinup issue, the HRLDAS control run was initialized with 1 January 2001 EDAS soil conditions to perform a continuous soil simulation until 1 July 2002, and 16 HRLDAS spinup experiments were conducted (see Table 3 for details). The averaged soil moisture, temperature, and fluxes for June 2002 from each HRLDAS spinup experiment were compared with those obtained from the control run with 17-month spinup up to 1 June 2002. For instance, the first HRLDAS spinup run was initialized with 1 February 2001 EDAS soil conditions and run from 1 February 2001 through 1 July 2002, yielding a run with 16 months of spinup to 1 June 2002 (1 month shorter than the control run). The second HRLDAS spinup run was initialized with 1 March 2001 EDAS soil conditions and run from 1 March 2001 through 1 July 2002, yielding a 15-month spinup, and so forth. The last (16th) HRLDAS spinup run was initialized with 1 June 2002 EDAS soil conditions and had no spinup for 1 June 2002.

Root-mean-square difference (RMSD) between the control run and each subsequent spinup run is computed at hourly output time interval during the month, and then the monthly mean of these hourly RMSDs is computed. These results are shown as a function of soil texture and lead time (months) in Figs. 3 and 4. The quasi-equilibrium criteria selected here are that 1) the June 2002 volumetric soil moisture RMSD is less than 0.02 and 2) the soil temperature RMSD is less than 0.5 K. It is obvious that the surface soil layer reaches quasi equilibrium more quickly than the deep root zone. The spinup time for soil moisture at the 5-cm soil layer is less than 1 month for most soil textures (Figs. 3a,c), and the spinup time for soil temperature at the 5-cm soil layer is about 4 months (Fig. 4a). For deep root zone soil moisture, the spinup time ranges from 4 (for sand) to more than 16 (for sandy clay loam) months, and it typically requires 13 months for most soil types to reach their quasi equilibrium. Coarser soil textures, which have larger soil hydraulic conductivities, take less time to spin up than do fine soil textures. Note that the midday RMSDs are slightly larger and require longer spinup times.

The ultimate goal for HRLDAS is to provide high-quality soil conditions to compute surface heat fluxes in coupled models. It is therefore necessary to examine how the differences in soil conditions translate into differences in surface fluxes during spinup. Because errors in coupled NWP models, in particular those of clouds and radiation, can easily lead to larger errors in surface heat fluxes than soil conditions, we assume that an RMS difference of 10 W m^{-2} is a reasonable quasi-equilibrium criterion for surface heat fluxes. As shown on Fig. 5, latent and sensible heat fluxes have similar spinup characteristics as a function of soil texture. Across soil texture (except the soil category 16 because of its small sample), the average spinup time for a

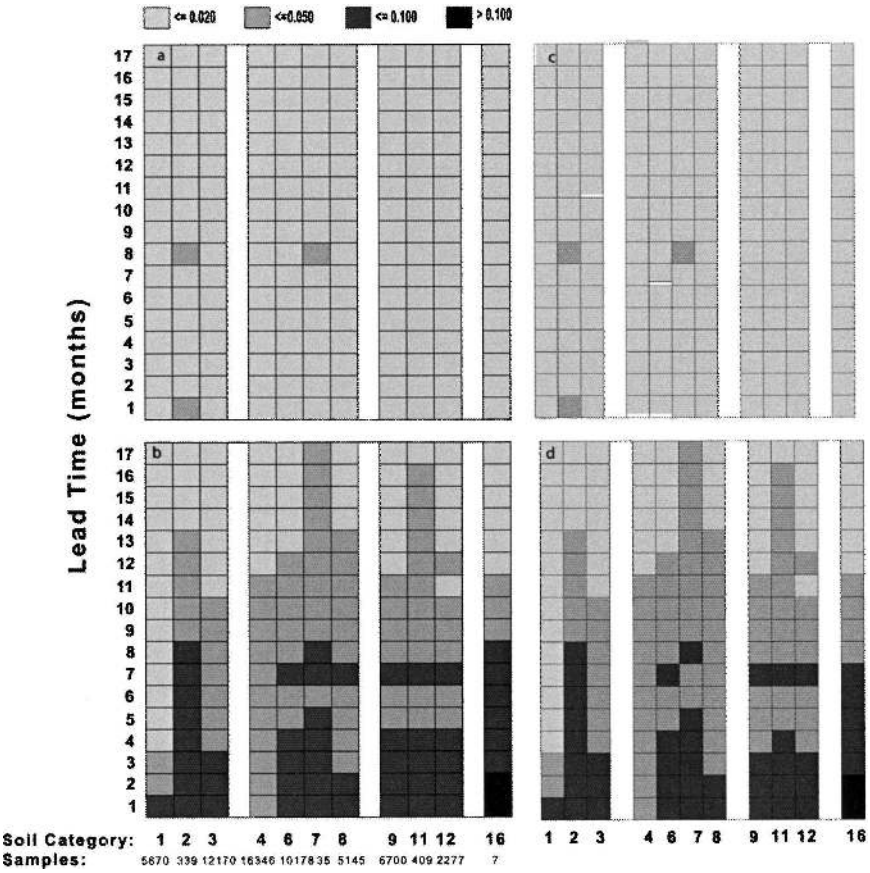

FIG. 3. RMS differences of volumetric soil moisture, computed as average for June 2002, between the HRLDAS control run and each HRLDAS spinup run: (a) soil moisture at 5-cm depth; (b) soil moisture at 70-cm depth; (c) same as (a), but for midday (1100–1400 LST) differences; and (d) same as (b), but for midday (1100–1400 LST) differences. Soil types found in this HRLDAS domain are classified into three groups of texture categories (within each group, the soil category numbers as shown in the figure are listed in parentheses after the soil-type names): (i) coarse soil textures, including sand (1), loamy sand (2), and sandy loam (3); (ii) medium soil textures, including silt loam (4), loam (6), sandy clay loam (7), and silty clay loam (8); and (iii) fine soil textures, including clay loam (9), silty clay (11), and clay (12). Soil texture category 16 is referred to as "other" in the State Soil Geographic Database (STATSGO, now referred to as the U.S. General Soil Map), and has only seven grid points in the 4-km HRLDAS domain.

quasi-equilibrium state is about 8 months for both surface fluxes, which is shorter than that for soil moisture and temperature. It took roughly 3–4 months to achieve surface flux variations of less than 15 W m^{-2}, which is not a far-fetched criterion for coupled NWP model applications, considering, again, uncertainty in the computation of radiation. As in the case of soil moisture/temperature spinup, the monthly averaged midday RMS differences are usually larger than the daily mean values. In this study, the spinup experiments are initialized from the land states of the EDAS, which uses the same four soil layers and very similar generation of the Noah LSM and assimilates stage-IV precipitation analyses, and hence cold-start initial land states will likely required longer spinup time as well. Also note that even though the IHOP_2002 domain investigated here comprises various land use types, the spinup would be different in the rugged orography region of the western contiguous United States (CONUS), where winter snowpack and frozen soil may play a big role in required spinup times.

b. Verification of atmospheric forcing conditions used in HRLDAS

Among the atmospheric forcing conditions used in HRLDAS, hourly precipitation and downward solar radiation play the primary roles in driving the land modeling system and determining long-term evolution of

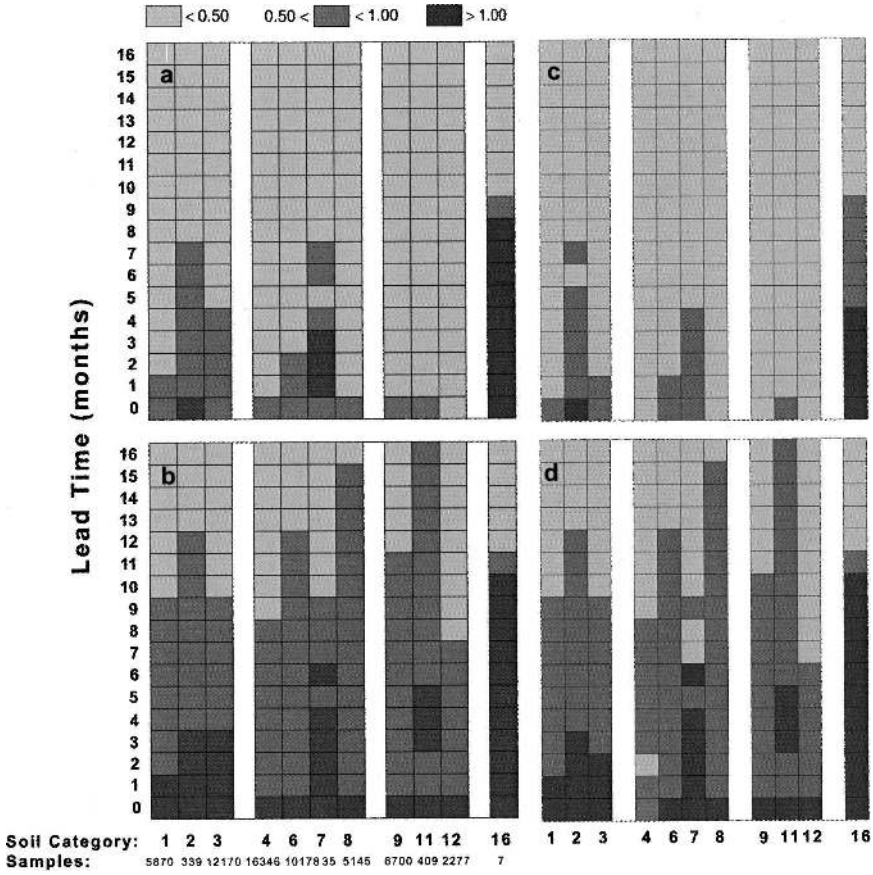

FIG. 4. As in Fig. 3, but for RMS differences of soil temperature (K).

soil moisture and temperature. Recent work of Cosgrove et al. (2003) and Luo et al. (2003) focused on verifying ⅛° NLDAS forcing conditions, and it is necessary for us to extend this kind of verification on the 4-km HRLDAS grid to understand whether the errors in forcing conditions depend on spatial scale. In contrast to the NLDAS verification efforts, the aspects investigated here include verification of hourly 4-km stage-IV rainfall products and monthly-averaged diurnal cycle of EDAS forcing. The precipitation verification of stage-IV rainfall was conducted using the IHOP_2002 rain gauge data at the 10 sites. Note that NLDAS uses the NCEP ¼° daily gauge-only precipitation analyses and the daily precipitation analysis is spatially interpolated to ⅛° and then temporally disaggregated into hourly fields by deriving hourly disaggregation weights from the hourly stage-IV rainfall. Luo et al. (2003) verified NLDAS ⅛° against Oklahoma Mesonet station data.

The hourly 4-km NCEP stage-IV rainfall compares, in general, well to IHOP_2002 surface station measurements (Fig. 6). For the relatively dry regions (i.e., at the western IHOP_2002 sites 1, 2, 3, and 10), the NCEP stage-IV rainfall slightly overestimated the rainfall while it underestimated rainfall for the transitional and wet regions, with the largest error for the IHOP_2002 site 8. It is not clear at this stage why the errors in the stage-IV rainfall analysis exhibit this spatial pattern. Nevertheless, note that the stage-IV product may not verify as well in the northern-tier CONUS states that have a longer winter season and more frozen precipitation (snowfall) or over the rugged western CONUS, because of greater frozen precipitation and mountain blocking of the radar beam.

During early morning and late-afternoon (i.e., low solar angle) 5-h periods, the GOES-derived solar radiation is largely overestimated. The average of RMSE for the rest of the day is about 80 W m^{-2}—typical RMSE values that are also observed in the evaluation of Pinker et al. (2003) when using hourly data. Bias in GOES-derived downward solar radiation is usually positive and less than 20 W m^{-2}. When compared with errors in satellite-derived downward solar radiation forcing, the errors in the EDAS downward longwave radiation are in general smaller and are negligible for land surface modeling purposes. Positive (negative)

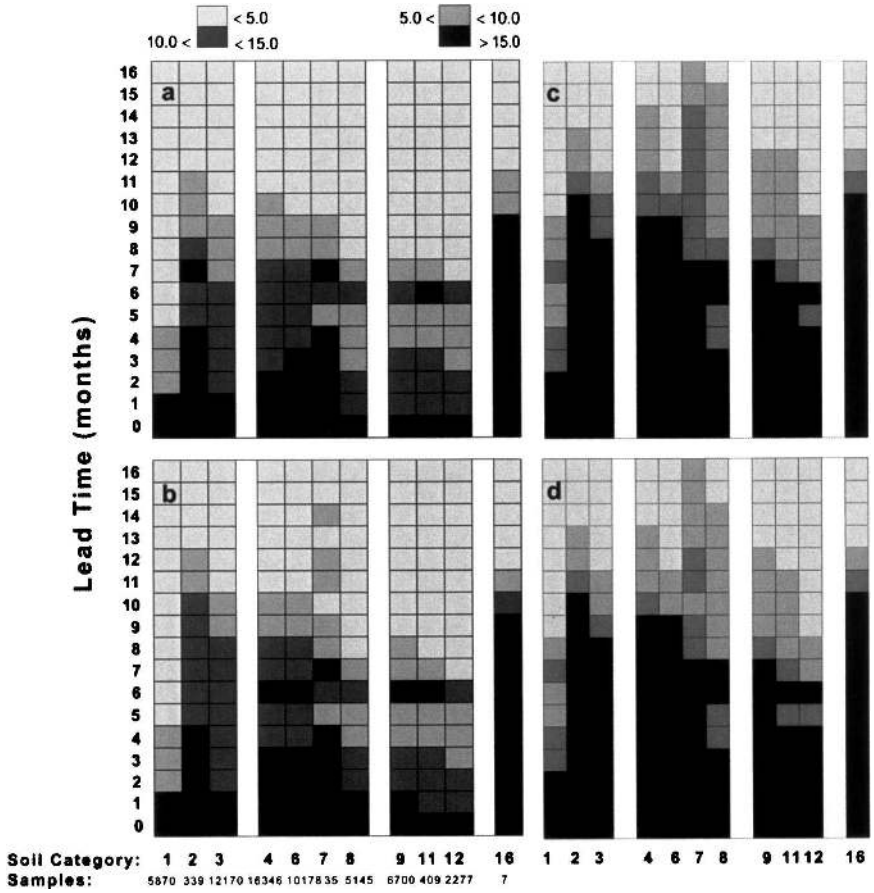

FIG. 5. Similar to Fig. 3, but for RMS differences of surface heat fluxes (W m^{-2}): (a) latent heat flux, (b) sensible heat flux, (c) midday (1100–1400 LST) latent heat flux, and (d) midday (1100–1400 LST) sensible heat flux.

bias in EDAS longwave radiation for daytime (nighttime) may reflect the overall air temperature bias in EDAS.

Surface wind, pressure, temperature, and humidity (which were obtained from the NCEP 40-km EDAS and interpolated on the HRLDAS 4-km grid) are compared with hourly Oklahoma Mesonet observations, roughly from 114 stations from 1 January to 30 June 2002, in Fig. 7. The RMSE (<6 hPa) and bias (systematically positive and <2 hPa) of surface pressure did not display a diurnal pattern, and the surface temperature, dewpoint temperature, and mixing ratio usually had low bias (high bias) for nighttime (daytime). Typical RMSE values ranged from 1.5 to 2.2 K for temperature and from 0.4 to 1.1 g kg^{-1} for mixing ratio and were roughly 1.4 m s^{-1} for wind speed. The errors in EDAS surface variables for wintertime are in general smaller. These error margins are reasonably accurate for use in this kind of long-term HRLDAS simulation, and the verification statistics found here using mesonet data are comparable to those from the evaluation of NLDAS against data from the Atmospheric Radiation Measurement Program Cloud and Radiation Test Bed by Luo et al. (2003).

c. *HRLDAS response to atmospheric forcing conditions*

This section discusses the degree to which long-term HRLDAS simulations respond to errors in forcing conditions. Qu et al. (1998) studied the sensitivity of latent heat flux to variations of surface air temperature, and Luo et al. (2003) used two sets of forcing conditions (NCEP EDAS and station observations) in NLDAS experiments to investigate differences in NLDAS output caused by differences in these two sets of forcing conditions. Nevertheless, the LSM response of surface heat fluxes, soil moisture, and soil temperature to each of the forcing variables has not been systematically explored in the past. We conducted a number of sensitivity tests to investigate HRLDAS sensitivity to each of

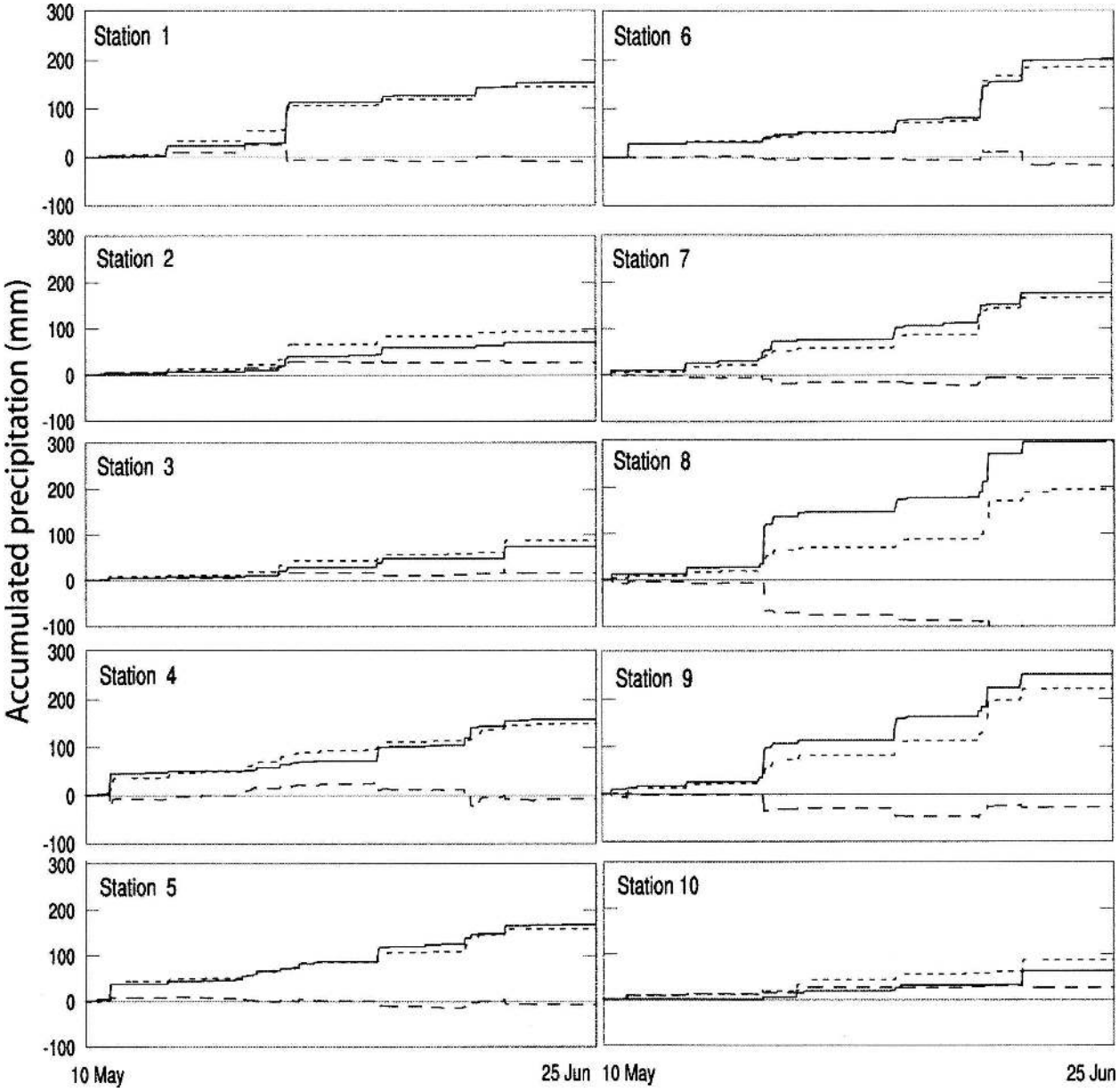

FIG. 6. Comparison of the total accumulated rain (mm) (with hourly time intervals) from 14 May to 25 Jun 2002 between stage-IV rainfall (short-dashed line) used in HRLDAS forcing and IHOP_2002 measurements (solid line) at each site. Long-dashed lines are accumulated errors (stage IV − IHOP) for the above period. Note that the accumulated error for site 8, being slightly out of the plotting scale, is −101.8 mm by the end of the period.

the forcing variables. In each sensitivity test, a typical bias value (based on forcing-error statistics described in section 3b) for a specific variable was used to perturb that variable used in each HRLDAS sensitivity run. For instance, air temperature is increased by 2 K (referred to as the "T+2" sensitivity experiment in Table 4) at each time step and each grid point for the 18-month sensitivity run, and the RMS differences and biases are computed between the control and sensitivity runs and then averaged for the last 3 months (i.e., April, May, and June 2002), assuming an equilibrium state was reached by then. Positive bias in forcing conditions generally produced 1) higher latent heat fluxes, 2) lower sensible heat fluxes (except for more solar downward radiation), and 3) lower soil moisture (except for more rain) as a result of larger surface evaporation, but more rain and stronger winds decreased soil temperature in the first soil layer. Positive bias in radiation, wind, and

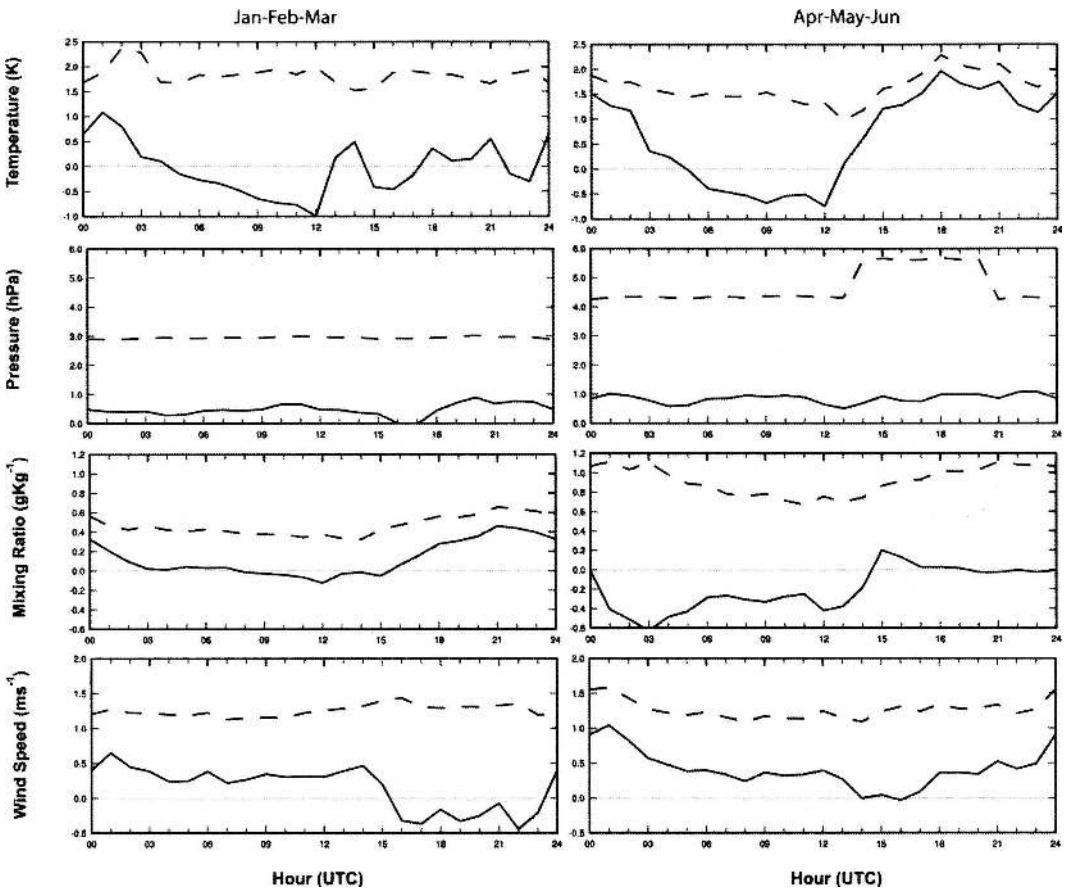

FIG. 7. RMSE (solid line) and bias (dashed line) of EDAS surface air temperature (K), pressure (hPa), mixing ratio (g kg^{-1}), and wind speed (m s^{-1}) computed with hourly Oklahoma Mesonet data and averaged for January–March and for April–June 2002.

temperature increases the daytime atmospheric surface layer instability (i.e., larger potential evaporation) so as to produce more evaporation and drier soils; more rain will produce more evaporation, less sensible heating, and wetter soils (referred to as the "Rn+20%" experiment in Table 4). Also note that the errors of rainfall are based on verification against IHOP_2002 data and that the precipitation forcing errors in a coupled data assimilation system can be substantially larger because of typically larger model-generated precipitation.

We found that, among various forcing variables, the HRLDAS is most sensitive to air temperature changes and least sensitive to wind speed changes. In other words, HRLDAS is more sensitive to air temperature errors for the typical bias range of each forcing variable, at least for the U.S. SGP region. Therefore, only these temperature and wind sensitivity test results plus those with rainfall and downward shortwave radiation (two important water and energy forcing conditions) are shown in Table 4. A typical error (e.g., 10% bias) in downward solar radiation produced similar but smaller changes in HRLDAS than did errors in temperature, and rainfall errors produced smaller changes than temperature and solar radiation.

Important is that changes of HRLDAS latent heat and sensible heat flux are not linear with respect to the change of air temperature, consistent with the work of Qu et al. (1998). For instance, decreasing air temperature in HRLDAS resulted in greater differences in surface fluxes and soil moisture than increasing air temperature, and similar results apply to other forcing variables. Downward shortwave radiation is the only exception in which HRLDAS is more sensitive to increasing radiation values, but the difference between the test with increasing 10% and the test with decreasing 10% is fairly small. Note that numerical sensitivity experiments conducted here assumed a systematic bias. In reality, however, the forcing may not always display a systematic bias across time and the spatial domain, and effects of positive bias in the forcing conditions on HRLDAS results could cancel out the effects of negative bias.

TABLE 4. RMSD and bias between control run and each sensitivity run. RMSD are first computed for each output time interval and then averaged for the last 3 months (May–July 2002) of simulations started at 1 Jan 2001 (SH: sensible heat flux; LH: latent heat flux; SM1: volumetric soil moisture of the first soil layer; SM3: volumetric soil moisture of the third soil layer; ST1: soil temperature of the first soil layer; ST3: soil temperature of the third soil layer; T+2: sensitivity run with air temperature increased by 2 K for each 30-min time step; T−2: sensitivity run with air temperature decreased by 2 K for each 30-min time step; Rn+20%: sensitivity run with rainfall amount increased by 20%; Rn−20%: sensitivity run with rainfall amount decreased by 20%; SW+10%: sensitivity run with downward shortwave radiation increased by 10%; SW−10%: sensitivity run with downward shortwave radiation decreased by 10%; SPD+20%: sensitivity run with wind speed increased by 20%; SPD−20%: sensitivity run with wind speed decreased by 20%.

	RMSD						Bias					
	SH	LH	SM1	SM3	ST1	ST3	SH	LH	SM1	SM3	ST1	ST3
	(W m^{-2})	(W m^{-2})	(%)	(%)	(K)	(K)	(W m^{-2})	(W m^{-2})	(%)	(%)	(K)	(K)
T+2	22.43	19.55	1.68	1.60	1.61	1.12	−17.69	7.90	1.58	−1.56	1.59	1.11
T−2	27.94	28.21	1.95	1.84	1.57	1.05	21.11	−11.62	1.83	1.82	−1.55	−1.04
Rn+20%	9.73	8.28	1.72	1.87	0.14	0.13	−5.65	5.70	1.70	1.84	−0.07	0.11
Rn−20%	15.97	14.19	2.47	2.85	0.25	0.19	9.21	−9.36	−2.42	−2.80	0.11	−0.16
SW+10%	21.88	10.79	0.90	0.82	0.26	0.09	14.04	6.12	−0.80	−0.77	0.22	0.08
SW−10%	20.77	12.61	0.87	0.79	0.26	0.09	−13.25	−6.93	0.79	0.76	−0.22	−0.08
SPD+20%	5.79	5.77	0.40	0.25	0.10	0.05	−0.30	0.60	−0.32	−0.24	−0.04	−0.05
SPD−20%	6.12	5.26	0.45	0.29	0.11	0.07	0.37	−0.74	0.36	0.29	0.05	0.06

d. Evaluation of HRLDAS surface latent and sensible fluxes

We are primarily interested in the performance of HRLDAS for the summer months, because we plan to use HRLDAS output for investigating summer boundary layer development and convection initiation. It is worth keeping in mind, though, that the HRLDAS output for the summer is a result of a long-term HRLDAS integration. The HRLDAS surface fluxes were compared with the monthly diurnal cycle of measured fluxes averaged for each site to obtain statistics (bias and RMSE). Many prior results (Twine et al. 2000; Yates et al. 2001) have shown the sum of sensible and latent heat fluxes measured by eddy covariance to be less than the difference between net radiation and soil heat fluxes. For instance, the residual, averaged for all Cooperative Atmosphere–Surface Exchange Study (CASES97) sites, in surface energy balance around solar noon was approximately 50 W m^{-2} (Yates et al. 2001), typically with the sum of surface fluxes always being smaller than the surface net radiation. These studies usually have neglected the heat storage in the canopy and energy associated with photosynthesis, but both probably are small for IHOP_2002. We can remove this problem for comparison with the HRLDAS results by assuming that the sensible heat fluxes are correct and synthesizing "budget" latent heat fluxes from the difference of net radiation plus soil heat fluxes and sensible heat fluxes. We acknowledge that adding the imbalance to the latent heat flux is an arbitrary choice and that the imbalance could be in any of the other three energy budget terms or in other terms, but this gives another measure, albeit not necessarily more accurate, of verification given the problem of KH2O sensor failure.

Table 5 documents the verification statistics (averaged for 14 May–25 June 2002) for each of the 10 IHOP_2002 stations. HRLDAS tends to have high bias in latent heat fluxes, and using the budget latent heat flux derived from the surface energy budget produced a better score, as expected. Simulated sensible heat flux compares to IHOP_2002 data better than does simulated latent heat flux, and the verification statistics computed from sensible heat flux may be more meaningful than those computed from latent heat fluxes, considering the problematic accuracy of the latter. That given, we believe HRLDAS still overestimates latent heat flux based on comparing with the budget data. In general, HRLDAS performed best for winter-wheat fields (sites 5 and 6) and worst for grassland (sites 7, 8, and 9). Its better performance for winter wheat is largely attributed to the relatively uniform distribution of winter wheat at small (field) scales. Note that winter wheat also had a distinct phenology—namely, being at its peak growing season from late April to middle-to-late May and being harvested at the middle of June. Vegetation fraction data used in HRLDAS seemed to capture this evolution well.

Figure 8 shows error statistics of HRLDAS sensible heat fluxes as verified with IHOP_2002 station data averaged for the period of 10 May–25 June 2002. RMSE and bias are within the error ranges of downward solar and longwave radiation forcing. Note that despite the high bias in wind speed, HRLDAS usually underestimated the negative nocturnal sensible heat flux. This is largely attributed to low biases in longwave

TABLE 5. RMSE and bias (W m^{-2}), averaged from 14 May to 25 Jun 2002, of HRLDAS latent heat flux (LH) and sensible heat flux (SH) verified against 10 IHOP_2002 surface station measurements. The LH below represent verification statistics using IHOP_2002 "original" latent heat flux data, and LH_budget are those using IHOP_2002 latent heat flux derived from the surface energy balance. Grass is averaged values for sites 2, 4, 7, 8 and 9; sparse is for sites 3 and 10; and wheat is for sites 5 and 6.

	RMSE			Bias		
Site	SH	LH	LH_budget	SH	LH	LH_budget
1	54.52	104.64	91.70	11.31	43.58	26.32
2	57.23	75.55	68.81	18.45	22.52	5.28
3	55.55	87.61	97.00	10.86	35.60	17.22
4	48.08	115.10	84.76	7.40	45.60	16.80
5	53.66	89.96	68.31	7.10	24.99	1.61
6	56.27	82.85	78.68	−5.08	24.46	16.80
7	45.45	206.10	87.44	3.72	114.85	18.79
8	42.15	208.20	120.21	5.35	111.98	33.02
9	52.29	179.77	131.58	−12.07	86.08	47.70
10	56.46	96.35	63.39	10.42	41.10	−3.11
Grass	49.04	156.95	98.56	4.58	76.21	24.32
Sparse	56.00	91.98	80.20	10.64	38.35	7.06
Wheat	54.97	86.41	73.50	1.01	24.72	9.20

radiation and surface air temperature, which enhanced the stability of the nighttime surface layer. It is not clear, nevertheless, why HRLDAS underestimated early morning sensible heat fluxes. HLRDAS overestimated latent heat fluxes even when compared with the budget latent heat flux (Fig. 9). In particular, HRLDAS produced erroneously large, nocturnal, negative (downward) latent heat fluxes, and the dew formation in the Noah LSM is certainly one problematic area that needs to be examined further.

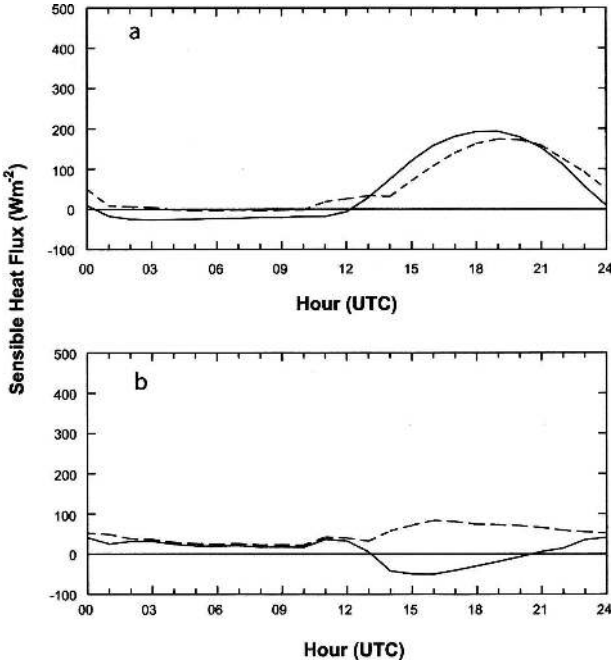

FIG. 8. Comparison of surface sensible heat fluxes (W m^{-2}) between HRLDAS and IHOP_2002 as averaged diurnal cycle from 14 May 2002 to 25 Jun 2002 and averaged for all 10 IHOP_2002 surface stations: (a) IHOP_2002 data (solid line) and HRLDAS (dashed line) and (b) bias (solid line) and RMSE (dashed line).

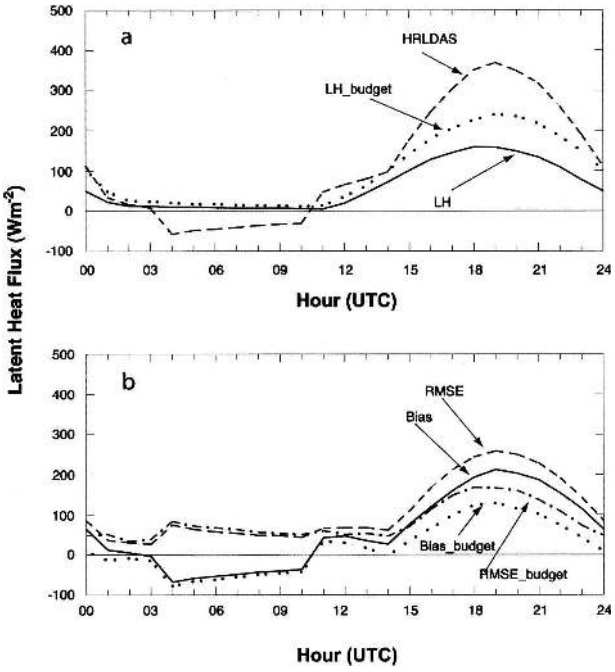

FIG. 9. As in Fig. 8, but for surface latent heat fluxes (W m^{-2}). (a) IHOP_2002 data (solid line), budget-derived IHOP_2002 latent heat flux (dotted line), and HRLDAS (dashed line); (b) bias computed using IHOP_2002 data (solid line), bias computed with budget-derived IHOP_2002 data (dotted line), RMSE computed with IHOP_2002 data (dashed line), and RMSE computed with budget IHOP_2002 data (dash–dot line).

e. Verification of soil moisture and temperature with the Oklahoma Mesonet data

Soil moisture and temperature measurements from the Oklahoma Mesonet were used to evaluate HRLDAS, because of the large number of sites (101 sites) and long time period for which soil data are available. We selected the period 1 April–26 June 2002 and removed sites with clear erroneous data, for example, sites with quasi-constant soil moisture data (i.e., measurement did seem to respond to rainfall) and sites with missing data for a long period. Model soil moisture has been verified against observations in the past using either total soil content for a soil layer (Robock et al. 1995; Chen and Mitchell 1999; Schaake et al. 2004) or volumetric soil moisture (Robock et al. 2003). We chose volumetric soil moisture for comparison in this study because the first (5 cm) and second (25 cm) soil layer

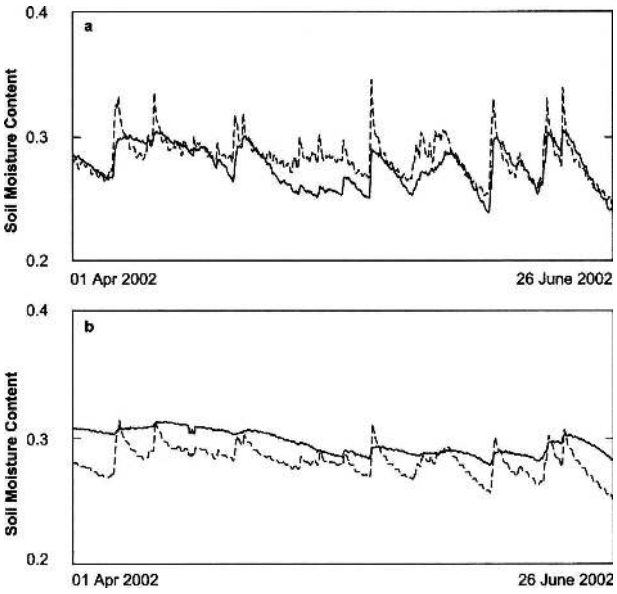

FIG. 10. Comparison of hourly volumetric soil moisture between HRLDAS and the Oklahoma Mesonet data, averaged over 30–65 mesonet stations: soil moisture at (a) 5 and (b) 25 cm for observations (solid line) and HRLDAS (dashed line).

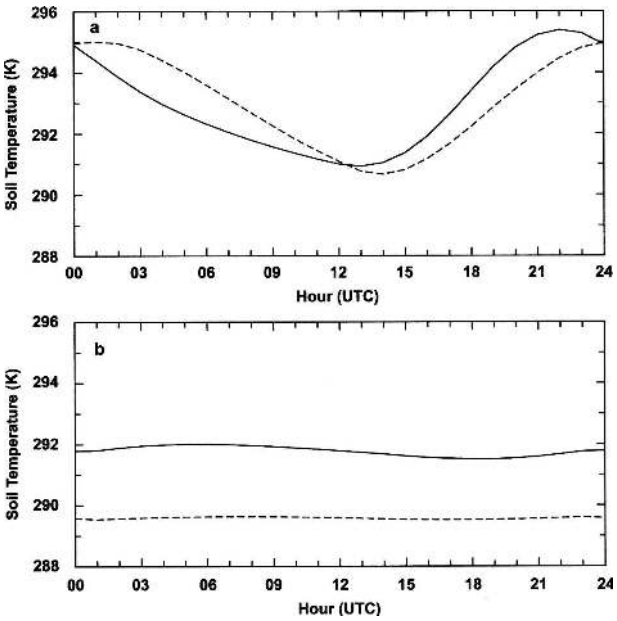

FIG. 11. As in Fig. 10, but for the diurnal cycle of soil temperature (K) averaged from 1 Apr to 26 Jun 2002.

depths in HRLDAS coincide with the mesonet soil measurement depths.

From early spring to early summer, the observed seasonal variability of surface volumetric soil moisture was small (Fig. 10), similar to mesonet soil moisture results of Robock et al. (2003). HRLDAS soil moisture has generally good agreement with mesonet observations, and the RMSE of volumetric soil moisture is 0.015 for the 5-cm layer and 0.018 for the 25-cm layer. However, HRLDAS produces slightly larger seasonal variation than observed, especially for the surface soil moisture, and has higher surface soil moisture (bias = 0.0075) and generally lower 25-cm soil moisture (bias = −0.15). Although many factors (e.g., precipitation forcing and HRLDAS evaporation parameterization) can contribute to this, a wetter surface layer and a drier deeper soil layer in HRLDAS may suggest a somewhat too low hydraulic conductivity parameterized by the Noah LSM. That probably can explain, at least in part, the high bias in HRLDAS latent heat flux shown in Table 5 and Fig. 9. Despite these discrepancies, HRLDAS was able to capture the observed seasonal tendency of soil moisture evolution. More important, there is no sign of severe drift of soil moisture after a 15-month continuous HRLDAS execution, indicating the generally good behavior of various forcing and robustness of HRLDAS.

Observed surface soil temperature exhibits large seasonal variability (roughly 20 K) and generally increased with time during that time span, with occasional cooling events due to the passage of large-scale weather systems (not shown). Again, HRLDAS captured the observed diurnal soil temperature variations reasonably well (RMSE = 1.74 K for 5-cm layer and 2.26 K for 25-cm layer; Fig. 11), owing to constraints in satellite-derived solar downward radiation and surface air temperature.

f. Development of small-scale heterogeneity in atmospheric low-level water vapor fields

Although the main purpose of HRLDAS is to provide accurate soil, surface, and vegetation conditions for initializing coupled mesoscale modeling systems, a number of HRLDAS-simulated fields such as surface evaporation and runoff can also be utilized for local and regional water budget studies. An IHOP_2002 case (25 May 2002) is used here to illustrate the degree to which the surface evaporation is related to the low-level water vapor field, when there is strong soil moisture heterogeneity due to a recent rainfall event. Furthermore, this particular case provides a novel opportunity to verify HRLDAS spatial distribution of latent heat flux (evaporation), because high-resolution water vapor fields for a relatively large domain derived from radar have only recently become available.

During IHOP_2002, the NCAR S-band dual-polarization radar (S-Pol), located in the Oklahoma Panhandle, collected high-resolution spatial and temporal measurements of near-surface moisture variabil-

ity using a radar refractivity technique developed by Fabry et al. (1997). This technique is based on the concept that variability in radar wave propagation between the radar and ground targets is due to changes in the properties of the air (i.e., changes in index of refraction) between the radar and the targets. Variability of index of refraction or refractivity N can be measured by the radar as a change in phase of the electromagnetic waves as they travel between the radar and the target. From Fabry et al. (1997), N can be calculated as

$$N = 77.6(P/T) + 3.73 \times 10^5(e/T^2), \quad (1)$$

which depends on pressure P (hPa), temperature T (K), and water vapor pressure e (hPa) to retrieve the near-surface water vapor estimates. Although the first term on the right (proportional to air density) is typically larger than the second (humidity) term, Fabry (2006) has found, using surface data, that most of the spatial variability in N is due to the variability in water vapor (75% of the total contribution) and less (24%) is due to temperature variability. Hence, the S-Pol refractivity measurements collected during IHOP_2002, when the contribution of temperature variability to N was small, represent approximations for near-surface moisture.

Comparison of the S-Pol refractivity fields with moisture measurements from the IHOP_2002 surface mesonet, low-flying aircraft, and other vertical profiling sensors show high correlations, validating the refractivity retrieval technique as a good approximation for humidity measurements in the lowest ~250 m of the boundary layer (Weckwerth et al. 2004). Figure 12 shows the evolution of both S-Pol radar-derived refractivity field and HRLDAS surface evaporation in the morning of 25 May 2002 for an area centered at the Oklahoma Panhandle. Refractivity is plotted rather than water vapor content, because the small contribution of temperature variability cannot be neglected or separated out. The S-Pol plot and HRLDAS plot employ slightly different map projections. However, the Kansas–Oklahoma and Oklahoma–Texas borderlines on the plots may be used as geographical references. The region was mostly cloud free throughout 25 May 2002, with a light southeast wind (roughly 2–5 m s^{-1}) in the morning. At 1200 UTC [0600 central standard time (CST)], before the surface evaporation became active (note that the maximum hourly evaporation was about 0.1 mm), low-level water vapor at 1200 UTC (0600 CST) was mostly uniform across the domain. The refractivity field started to develop a maximum [which, from Eq. (1), is also a maximum in mixing ratio] approximately 25 km south-southeast of the radar by 1600 UTC (1000 CST). This maximum corresponds to an area of large evaporation in HRLDAS, which is associated with wet soils, resulting from up to 50 mm of rain in the early hours of 24 May (Fabry 2006). This kind of heterogeneity in water vapor over the S-Pol domain continued to increase throughout the morning (because of surface drying in the northwest quarter of the region) and eventually formed a northeast–southwest-oriented corridor of high moisture that, again, seemed to be determined by local heterogeneity in soil moisture and surface evaporation.

4. Summary

The HRLDAS, based on the Noah LSM, has been developed at NCAR to meet the increasingly challenging demand for high-resolution, accurate land-state fields required to initialize coupled NWP–LSM models. It was designed to integrate 1) high-resolution atmospheric forcing conditions (e.g., 4-km rainfall), 2) baseline 1-km land use and soil texture maps, and 3) seasonally varying vegetation density that currently uses 0.15° climatological monthly data and can be easily replaced with future data such as Moderate-Resolution Imaging Spectroradiometer (MODIS)-derived LAI and green vegetation fraction with higher temporal and spatial resolution.

Both the uncoupled HRLDAS and WRF–Noah coupled models are executed on the same nesting grids 1) to capture high-resolution surface heterogeneity; 2) to eliminate mismatch in land surface model, terrain height, land use, soil texture, and LSM parameters to ensure the same soil climatological regime between the HRLDAS and WRF–Noah modeling systems; and 3) to reduce computational requirements. Nevertheless, for an uncoupled system like HRLDAS to generate the same evolution of land states and surface fluxes as the associated coupled model, it may be necessary but not sufficient that the HRLDAS use the same land model, the same terrain/land use/soil texture fields, and the same parameters as the associated coupled model. In fact, the uncoupled system may need also to be forced from the variables obtained from the lowest active model layer of the coupled system, rather than the diagnostic 2- and 10-m fields, because differences in the applicable vertical height and temporal frequency of the surface forcing and in the treatment of surface layer between the uncoupled and coupled systems may result in differences in the underlying climatological values and evolution of the land states and fluxes. This issue has not yet been sufficiently explored and needs further attention.

There were recent, collective efforts devoted to the development of the multi-LSM-based ⅛° NLDAS

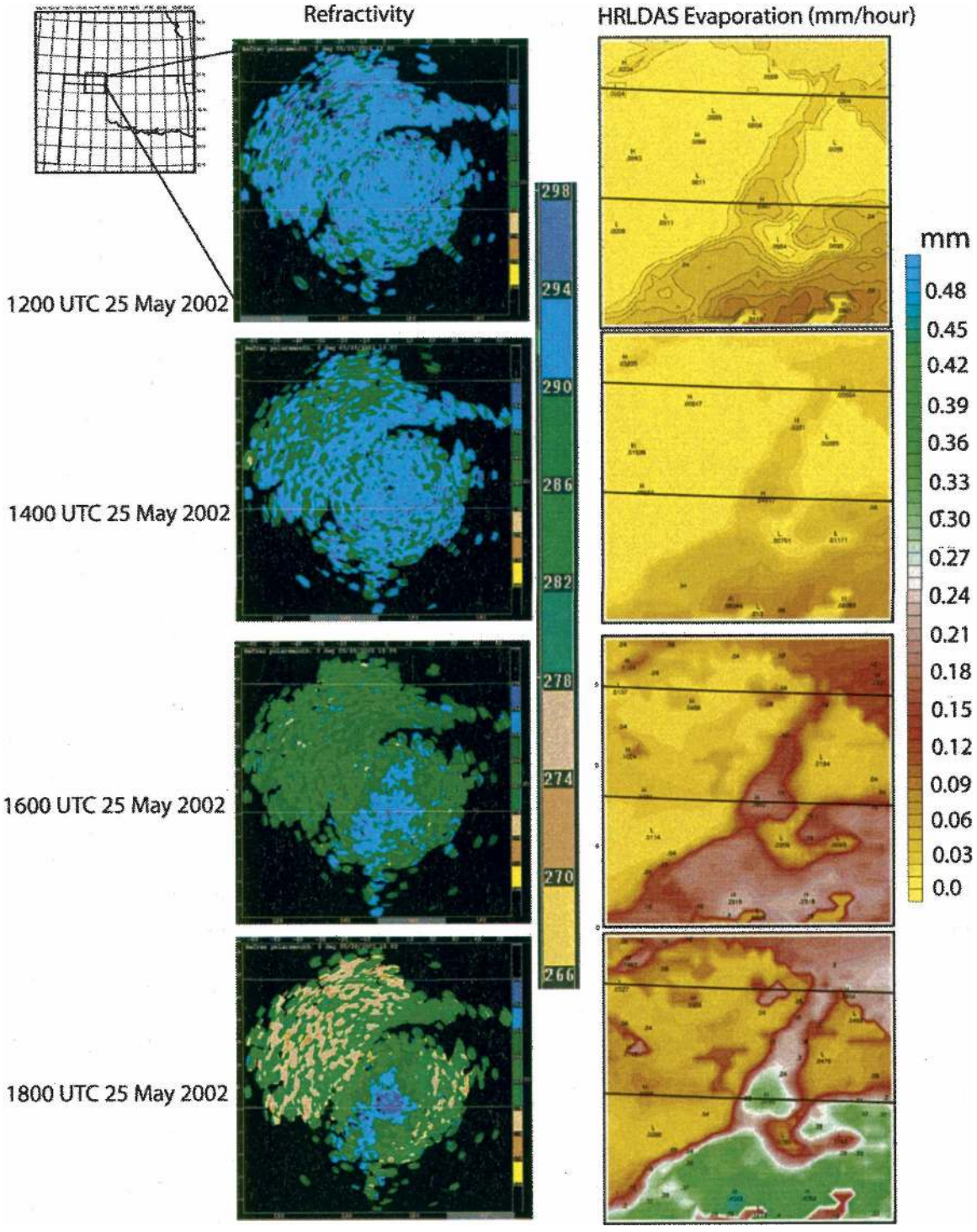

FIG. 12. Comparison between HRLDAS hourly surface evaporation (mm) and low-level water vapor (refractivity, N) derived from NCAR S-Pol radar, valid at 1200, 1400, 1600, and 1800 UTC 25 May 2002. A change of $4N$ is approximately equivalent to a 1 g kg^{-1} change in water vapor. Blue and green shades represent regions of higher moisture.

(Cosgrove et al. 2003; Robock et al. 2003; Pinker et al. 2003; Luo et al. 2003; Schaake et al. 2004; Mitchell et al. 2004; etc.). In comparison with those studies, our research effort consists of investigating, with a long-term (1 January 2001–30 June 2002) HRLDAS run with 12- and 4-km grid spacing, a few unique aspects of HRLDAS, including an analysis of its spinup dependency on soil texture, using previously spunup initial soil fields and surface heat flux as equilibrium criteria, an analysis of its sensitivity to each atmospheric forcing, and an evaluation of the characteristics of simulated soil fields and surface heat fluxes at 4-km scales.

Using changes in soil moisture and temperature as a traditional and yet somewhat arbitrary criterion, HRLDAS would need about 12 months to attain a quasi-equilibrium state. However, a more meaningful criterion may be the evolution of surface heat flux during the spinup, because soil moisture and temperature are ultimately translated into surface heat fluxes as lower boundary conditions for NWP models. It took only 3–4 months for HRLDAS, initialized with already spun up but coarser-resolution EDAS soil fields, to reach a state in which changes in both latent and sensible heat flux are less than 15 W m^{-2}. In pragmatic terms, this is a reasonable criterion considering errors in NWP-modeled surface radiation that can easily offset the uncertainty in soil moisture and temperature. This has important implications for NWP applications, because it is fairly common practice to change model configurations, especially horizontal resolution, to meet different requirements, and using previously spunup land-state fields obtained from a similar LDAS of moderately different spatial resolution probably would not require a long additional spinup time.

Atmospheric forcing conditions obtained from NCEP EDAS surface fields are impressively accurate, with the largest errors found in satellite-derived downward solar radiation, which is a difficult parameter to obtain owing to the small-scale nature of summer cumulus. Nevertheless, these solar radiation errors are randomly distributed to yield small biases. Upon examining a series of sensitivity tests, we found that atmospheric forcing-condition errors usually resulted in differences of less than 30 W m^{-2} for both HRLDAS latent and sensible heat fluxes. Evaluated against measurements from the 10 IHOP_2002 surface stations, HRLDAS had the best performance for winter-wheat stations, presumably because of the well-defined evolution of green vegetation cover of wheat during late spring and early summer. Therefore, incorporating future satellite data with higher temporal and spatial resolution, such as MODIS data, will improve the specification of these vegetation characteristics.

More important, HRLDAS-simulated soil moisture appears to be able to capture finescale heterogeneity in surface evaporation and low-level water vapor distribution. For the 25 May 2002 IHOP_2002 case, in which there were no large-scale synoptic systems and surface winds were light to moderate, the evolution of large water vapor in a concentrated area appeared to be determined by the morning soil moisture distribution and associated evaporation processes. HRLDAS is still in an early development stage and needs further improvements with regard to model physics and incorporation of new satellite data. Nevertheless, recent studies that used HRLDAS-generated land-state variables in mesoscale models (Trier et al. 2004; Holt et al. 2006) demonstrate its promising ability to capture impacts of finescale soil heterogeneity on summertime deep convection initiation.

Acknowledgments. The authors are grateful to Ken Mitchell (NCEP/EMC) for his thoughtful review, suggestions, and discussions, which led to improvements in this manuscript. We also thank two anonymous referees for their valuable comments. This research and development effort was supported by U.S. Weather Research Program (USWRP) Grant NSF 01, the U.S. Army Test and Evaluation Command, and the U.S. Air Force Weather Agency through an Interagency Agreement with the National Science Foundation (NSF), the NCAR TIIMES Water Cycle Program, NSF Grants ATM-0233780 and ATM-0236885, and NASA–THP Grants NNG04GI84G and NNG06GH17G.

REFERENCES

Basara, J. B., and T. M. Crawford, 2000: Improved installation procedures for deep layer soil moisture measurements. *J. Atmos. Oceanic Technol.,* **17,** 879–884.

——, and K. C. Crawford, 2002: Linear relationships between root-zone soil moisture and atmospheric processes in the planetary boundary layer. *J. Geophys. Res.,* **107,** 4274, doi:10.1029/2001JD000633.

Beljaars, A. C. M., P. Viterbo, M. Miller, and A. Betts, 1996: The anomalous rainfall over the United States during July 1993: Sensitivity to land surface parameterization and soil moisture anomalies. *Mon. Wea. Rev.,* **124,** 362–383.

Betts, A., F. Chen, K. Mitchell, and Z. Janjic, 1997: Assessment of the land surface and boundary layer models in two operational versions of the NCEP Eta Model using FIFE data. *Mon. Wea. Rev.,* **125,** 2896–2915.

Brock, F. V., K. C. Crawford, R. L. Elliott, G. W. Cuperus, S. J. Stadler, H. L. Johnson, and M. D. Eilts, 1995: The Oklahoma Mesonet: A technical overview. *J. Atmos. Oceanic Technol.,* **12,** 5–19.

Camillo, P. J., and T. J. Schmugge, 1983: Estimating soil moisture storage in the root zone from surface measurements. *Soil Sci.,* **135,** 245–264.

Chen, F., and K. Mitchell, 1999: Using GEWEX/ISLSCP forcing

data to simulate global soil moisture fields and hydrological cycle for 1987–1988. *J. Meteor. Soc. Japan,* **77,** 1–16.

——, and J. Dudhia, 2001: Coupling an advanced land surface–hydrology model with the Penn State–NCAR MM5 modeling system. Part I: Model implementation and sensitivity. *Mon. Wea. Rev.,* **129,** 569–585.

——, and Coauthors, 1996: Modeling of land-surface evaporation by four schemes and comparison with FIFE observations. *J. Geophys. Res.,* **101,** 7251–7268.

——, Z. Janjic, and K. Mitchell, 1997: Impact of atmospheric surface layer parameterization in the new land-surface scheme of the NCEP Mesoscale Eta numerical model. *Bound.-Layer Meteor.,* **l85,** 391-421.

——, T. Warner, and K. Manning, 2001: Sensitivity of orographic moist convection to landscape variability: A study of the Buffalo Creek, Colorado, flash-flood case of 1996. *J. Atmos. Sci.,* **58,** 3204–3223.

Cosgrove, B. A., and Coauthors, 2003: Land surface model spin-up behavior in the North American land data assimilation system (NLDAS). *J. Geophys. Res.,* **108,** 8845, doi:10.1029/2002JD003316.

Ek, M. B., K. E. Mitchell, Y. Lin, E. Rogers, P. Grummann, V. Koren, G. Gayno, and J. D. Tarpley, 2003: Implementation of Noah land surface model advances in the National Centers for Environmental Prediction operational Mesoscale Eta Model. *J. Geophys. Res.,* **108,** 8851, doi:10.1029/2002JD003296.

Entekhabi, D., H. Nakamura, and E. G. Njoku, 1994: Solving the inverse problem for soil moisture and temperature profiles by sequential assimilation of multifrequency remotely sensed observations. *IEEE Trans. Geosci. Remote Sens.,* **l32,** 438–448.

Fabry, F., 2006: The spatial variability of moisture in the boundary layer and its effect on convection initiation: Project-long characterization. *Mon. Wea. Rev.,* **134,** 79–91.

——, C. Frush, I. Zawadzki, and A. Kilambi, 1997: On the extraction of near-surface index of refraction using radar phase measurements from ground targets. *J. Atmos. Oceanic Technol.,* **14,** 978–987.

Fulton, R. A., J. P. Breidenbach, D.-J. Seo, D. A. Miller, and T. O'Bannon, 1998: The WSR-88D rainfall algorithm. *Wea. Forecasting,* **13,** 377–395.

Gayno, G., and J. Wegiel, 2000: Incorporating global real-time surface fields into MM5 at the Air Force Weather Agency. Preprints, *10th Penn State/NCAR MM5 Users' Workshop,* Boulder, CO, NCAR, 62–65.

Gutman, G., and A. Ignatov, 1998: The derivation of green vegetation fraction from NOAA/AVHRR data for use in numerical weather prediction models. *Int. J. Remote Sens.,* **19,** 1533–1543.

Holt, T., D. Niyogi, F. Chen, K. Manning, M. LeMone, and A. Qureshi, 2006: Effect of land–atmosphere interactions on the IHOP 24–25 May 2002 convection case. *Mon. Wea. Rev.,* **134,** 113–133.

Horst, T. W., 2006: Attenuation of scalar fluxes measured with horizontally-displaced sensors. *Proc. 17th Symp. on Boundary Layers and Turbulence,* San Diego, CA, Amer. Meteor. Soc., CD-ROM, 7.5.

Houser, P. R., W. J. Shuttleworth, J. S. Famiglietti, H. V. Gupta, K. H. Syed, and D. C. Goodrich, 1998: Integration of soil moisture remote sensing and hydrologic modeling using data assimilation. *Water Resour. Res.,* **34,** 3405–3420.

Jackson, T. J., 1980: Profile soil moisture from surface measurements. *J. Irrig. Drain. Div. Proc. ASCE,* **106,** 81–92.

——, 1997: Soil moisture estimation using Special Sensor Microwave/Imager satellite data over a grassland region. *Water Resour. Res.,* **18,** 1475–1484.

Jacquemin, B., and J. Noilhan, 1990: Sensitivity study and validation of a land surface parameterization using the HAPEX-MOBILHY data set. *Bound.-Layer Meteor.,* **52,** 93–134.

Koren, V., J. Schaake, K. Mitchell, Q.-Y. Duan, and F. Chen, 1999: A parameterization of snowpack and frozen ground intended for NCEP weather and climate models. *J. Geophys. Res.,* **104,** 19 569–19 585.

Koster, R., and C. P. Milly, 1997: The interplay between transpiration and runoff formulations in land surface schemes used with atmospheric models. *J. Climate,* **10,** 1578–1591.

Lanicci, J. M., T. N. Carlson, and T. T. Warner, 1987: Sensitivity of the Great Plains severe-storm environment to soil-moisture distribution. *Mon. Wea. Rev.,* **115,** 2660–2673.

Loveland, T. R., J. W. Merchant, J. F. Brown, D. O. Ohlen, B. C. Reed, P. Olson, and J. Hutchinson, 1995: Seasonal land-cover regions of the United States. *Ann. Assoc. Amer. Geogr.,* **85,** 339–355.

Luo, L., and Coauthors, 2003: Validation of the North American land data assimilation system (NLDAS) retrospective forcing over the southern Great Plains. *J. Geophys. Res.,* **108,** 8843, doi:10.1029/2002JD003246.

Mahrt, L., and K. Ek, 1984: The influence of atmospheric stability on potential evaporation. *J. Climate Appl. Meteor.,* **23,** 222–234.

——, and H. L. Pan, 1984: A two-layer model of soil hydrology. *Bound.-Layer Meteor.,* **29,** 1–20.

Miller, D. A., and R. A. White, 1998: A conterminous United States multilayer soil characteristics data set for regional climate and hydrology modeling. *Earth Interactions,* **2**. [Available online at http://EarthInteractions.org.]

Mitchell, K. E., and Coauthors, 2004: The multi-institution North American land data assimilation system (NLDAS): Utilizing multiple GCIP products and partners in a continental distributed hydrological modeling system. *J. Geophys. Res.,* **109,** D07S90, doi:10.1029/2003JD003823.

Noilhan, J., and S. Planton, 1989: A simple parameterization of land surface processes for meteorological models. *Mon. Wea. Rev.,* **117,** 536–549.

Pan, H.-L., and L. Mahrt, 1987: Interaction between soil hydrology and boundary-layer development. *Bound.-Layer Meteor.,* **38,** 185–202.

Pielke, R. A., Sr., and X. Zeng, 1989: Influence on severe storm development of irrigated land. *Natl. Wea. Dig.,* **14,** 16–17.

Pinker, R. T., and Coauthors, 2003: Surface radiation budgets in support of the GEWEX Continental Scale International Project (GCIP) and the GEWEX Americas Prediction Project (GAPP), including the North American Land Data Assimilation System (NLDAS) Project. *J. Geophys. Res.,* **108,** 8844, doi:10.1029/2002JD003301.

Qu, W., and Coauthors, 1998: Sensitivity of latent heat flux from PILPS land-surface schemes to perturbations of surface air temperature. *J. Atmos. Sci.,* **55,** 1909–1927.

Robock, A., K. Y. Vinnikov, C. A. Schlosser, N. A. Speranskaya, and Y. Xue, 1995: Use of midlatitude soil moisture and meteorological observations to validate soil moisture simulations with biosphere and bucket models. *J. Climate,* **8,** 15–35.

——, A. Schlosser, K. Vinnikov, N. Speranskaya, and J. Entin,

1998: Evaluation of AMIP soil moisture simulations. *Global Planet. Change,* **19,** 181–208.

——, and Coauthors, 2003: Evaluation of the North American Land Data Assimilation System over the southern Great Plains during the warm season. *J. Geophys. Res.,* **108,** 8846, doi:10.1029/2002JD003245.

Rogers, E., D. G. Deaven, and G. J. DiMego, 1995: The regional analysis system for the operational "early" Eta model: Original 80-km configuration and recent changes. *Wea. Forecasting,* **10,** 810–825.

Schaake J. C., and Coauthors, 2004: An intercomparison of soil moisture fields in the North American land data assimilation system (NLDAS). *J. Geophys. Res.,* **109,** D01S90, doi:10.1029/2002JD003309.

Shafer, M. A., C. A. Fiebrich, D. S. Arndt, S. E. Fredrickson, and T. W. Hughes, 2000: Quality assurance procedures in the Oklahoma Mesonet. *J. Atmos. Oceanic Technol.,* **17,** 474–494.

Shaw, B. L., R. A. Pielke, and C. L. Ziegler, 1997: A three-dimensional numerical simulation of a Great Plains dryline. *Mon. Wea. Rev.,* **125,** 1489–1506.

Tewari, M., and Coauthors, 2005: Numerical experiments with upgraded WRF/NoahLSM model. Preprints, *19th Conf. on Hydrology,* San Diego, CA, Amer. Meteor. Soc., CD-ROM, 4.10.

Trier, S. B., F. Chen, and K. W. Manning, 2004: A study of convection initiation in a mesoscale model using high-resolution land surface initial conditions. *Mon. Wea. Rev.,* **132,** 2954–2976.

Twine, T. E., and Coauthors, 2000: Correcting eddy-convariance flux underestimates over a grassland. *Agric. For. Meteor.,* **103,** 279–300.

Walker, J. P., and P. R. Houser, 2001: A methodology for initializing soil moisture in a global climate model: Assimilation of near-surface soil moisture observations. *J. Geophys. Res.,* **106,** 11 761–11 774.

Webb, E. K., G. I. Pearman, and R. Leuning, 1980: Correction of flux measurements for density effects due to heat and water vapor transfer. *Quart. J. Roy. Meteor. Soc.,* **106,** 85–100.

Weckwerth, T. M., and Coauthors, 2004: Overview of the International H2O Project (IHOP_2002) and some preliminary highlights. *Bull. Amer. Meteor. Soc.,* **85,** 253–277.

Wilczak, J., S. Oncley, and S. A. Stage, 2001: Sonic anemometer tilt correction algorithms. *Bound.-Layer Meteor.,* **99,** 127–150.

Yang, Z.-L., R. E. Dickinson, A. Henderson-Sellers, and A. J. Pitman, 1995: Preliminary study of spinup processes in land surface models with the first stage data of Project for Intercomparison of Land Surface Parameterization Schemes Phase 1(a). *J. Geophys. Res.,* **100** (D8), 16 553–16 578.

Yates, D. N., F. Chen, M. A. LeMone, R. Qualls, S. P. Oncley, R. Grossman, and E. A. Brandes, 2001: A Cooperative Atmosphere–Surface Exchange Study (CASES) dataset for analyzing and parameterizing the effects of land surface heterogeneity on area-averaged surface heat fluxes. *J. Appl. Meteor.,* **40,** 921–937.

Ziegler, C. L., T. J. Lee, and R. A. Pielke Sr., 1997: Convective initiation at the dryline: A modeling study. *Mon. Wea. Rev.,* **125,** 1001–1026.